AWARD NUMBER: W81XWH-19-1-0475

TITLE: Biofabrication of Cell-Decorated Telocollagen Fibers of Extraordinary Strength for Regenerative Tendon and Myotendinous Junction Repair

PRINCIPAL INVESTIGATOR: **Dr. Michael Francis**

CONTRACTING ORGANIZATION: EMBODY, INC.
JEFFREY CONROY
4111 MONARCH WAY STE 409
NORFOLK VA 23508-2563

REPORT DATE: August 2021

TYPE OF REPORT: Annual Technical Report

PREPARED FOR: U.S. Army Medical Research and Materiel Command
Fort Detrick, Maryland 21702-5012

REPORT DOCUMENTATION PAGE

Form Approved
OMB No. 0704-0188

1. REPORT DATE	2. REPORT TYPE	3. DATES COVERED
August 2021	Annual Technical Report	15 July 2020 – 14 July 2021

4. TITLE AND SUBTITLE
Biofabrication of Cell-Decorated Telocollagen Fibers of Extraordinary Strength for Regenerative Tendon and Myotendinous Junction Repair

5a. CONTRACT NUMBER
W81XWH-19-1-0475

5b. GRANT NUMBER
W81XWH-19-1-0475

5c. PROGRAM ELEMENT NUMBER

6. AUTHOR(S)
Kyle Christensen, PhD*; Michael Francis, PhD; Yas Maghdouri-White, PhD; Nardos Sori, PhD

*Corresponding author E-Mail: kchristensen@embody-inc.com

5d. PROJECT NUMBER
0011332768

5e. TASK NUMBER

5f. WORK UNIT NUMBER

7. PERFORMING ORGANIZATION NAME(S) AND ADDRESS(ES)
EMBODY, INC.
JEFFREY CONROY
4111 MONARCH WAY STE 409
NORFOLK VA 23508-2563

8. PERFORMING ORGANIZATION REPORT NUMBER

9. SPONSORING / MONITORING AGENCY NAME(S) AND ADDRESS(ES)
U.S. Army Medical Research and Development Command
Fort Detrick, Maryland 21702-5012

10. SPONSOR/MONITOR'S ACRONYM(S)
USAMRDC

11. SPONSOR/MONITOR'S REPORT NUMBER(S)

12. DISTRIBUTION / AVAILABILITY STATEMENT
Approved for Public Release; Distribution Unlimited

13. SUPPLEMENTARY NOTES

14. ABSTRACT
Musculoskeletal tissue injuries, including those occurring at the myotendinous junction (MTJ), are the leading cause for medical encounters for warfighters. Nonsurgical treatments and leading clinical repair scaffolds have significant limitations. To address this need, we developed a novel biomanufacturing, or 3D bioprinting, approach to produce strong, cellularized, living biomimetic grafts. Our bioprinting process utilizes strong clinical grade collagen microfibers and was optimized to controllably produce grafts with designed geometries and cellular distributions throughout. Printed grafts offer excellent biocompatibility, functional architectures, high cell viability, and mechanical properties mimicking those of native tendon. In all, this technology greatly outperforms previously developed tissue engineering approaches for producing biomimetic grafts with potential to improve the repair and regeneration of musculoskeletal and MTJ tissue injuries.

15. SUBJECT TERMS
Collagen, additive manufacturing, biomanufacturing, bioprinting, microfiber, biomimicry, myotendinous junction

16. SECURITY CLASSIFICATION OF:			17. LIMITATION OF ABSTRACT	18. NUMBER OF PAGES	19a. NAME OF RESPONSIBLE PERSON
a. REPORT	b. ABSTRACT	c. THIS PAGE			USAMRDC
Unclassified	Unclassified	Unclassified	Unclassified	31	19b. TELEPHONE NUMBER *(include area code)*

TABLE OF CONTENTS

1. INTRODUCTION:

Musculoskeletal tissue injuries, including those at the myotendinous junction (MTJ), are the leading cause for all medical encounters for warfighters at ~2 million cases per year, with extremity injuries accounting for up to 79% of trauma cases in theater. Available therapies have significant limitations, such that various tissue engineering approaches have been explored for the on-demand fabrication of living grafts for the treatment of these injuries. Recreating the structural, biochemical, and mechanical likeness of native tissue in an automated, scalable fabrication process has remained a challenge. Addressing these shortcomings, a novel biomanufacturing process was developed herein as a versatile and capable approach to produce therapeutic grafts with the potential to treat tendon/ligament and MTJ-related injuries. Produced grafts were assessed for their geometric fidelity, biocompatibility, cellularity, and mechanical properties and were found to mimic key aspects of native musculoskeletal tissue. Studies are underway to determine synthetic tissue development *in vitro* using bioreactor culture and regeneration of functional tissue *in vivo* in an animal defect model. It's envisioned that this platform biomanufacturing technology can produce cellularized grafts which promote and accelerate regeneration and functional recovery in debilitating musculoskeletal tissue injuries affecting Warfighters and civilians alike.

2. KEYWORDS:

Collagen, additive manufacturing, biomanufacturing, 3D bioprinting, microfiber, biomimicry, myotendinous junction

3. ACCOMPLISHMENTS:

What were the major goals of the project?

Objective 1: Bioprinting of strong and stable collagen microfibers decorated with viable cells.

Major Task 1: Design, build and test robust printheads for controllable high-output cell decorated collagen fiber grafts to mimic native tendon tissue strength and cellular arrangement.

Subtask 1: Design custom printhead to fit our commercial Folger Tech FT-5 R2 Large Scale 3D Printer.
Timeline (month of project): 1-4
Percent completion: 100%

Subtask 2: Regulatory approvals for the use of human mesenchymal stem cells (hMSCs) (RoosterBio) by HRPO.
Timeline (month of project): 1-3
Percent completion: 100%

Subtask 3: Generate sterile, crosslinked collagen fibers and culture research grade hMSCs (RoosterBio) for use in the 3D bioprinter.
Timeline (month of project): 4
Percent completion: 100%

Subtask 4: Create test scaffolds by feeding collagen fibers through the printhead, into the seeding reservoir with research grade MSCs (RoosterBio) and onto the build space.

Timeline (month of project): 5-8
Percent completion: 100%

Subtask 5: Assess test scaffolds for cell distribution, viability and mechanical strength

Timeline (month of project): 9
Percent completion: 100%

Subtask 6: Optimize process parameters (flow and draw rates, cell density and hyaluronic acid concentration) for optimal cell decoration on fibers using sterilized microfluidic collagen fibers and clinical grade MSCs (RoosterBio).

Timeline (month of project): 10-11
Percent completion: 100%

Subtask 7: Build repeating benchmark scaffolds using collagen fibers and MSCs to create test articles for 3D bioprinter performance validation.

Timeline (month of project): 11
Percent completion: 100%

Subtask 8: Finalize performance validation by testing benchmark scaffolds for cell distribution and viability, cellular metabolic activity and strength.

Timeline (month of project): 12
Percent completion: 100%

Subtask 9: IACUC and ACURO approval

Timeline (month of project): 4-9.
Percent completion: 100%

Objective 2: Bioreactor culture of cell-decorated collagen microfibers to study synthetic tissue development.

Major Task 2: Grow biomanufactured cell-decorated collagen fibers under cyclic tension in bioreactor cultures and compare to static cultures for strength, cellular arrangement and gene expression.

Subtask 1: Generate sterile, 3D bioprinted crosslinked collagen fibers with and without clinical grade human MSCs (RoosterBio) for use in bioreactor studies.

Timeline (month of project): 13
Percent completion: 100%

Subtask 2: Optimize bioreactor culture process parameters using cellular and acellular collagen fiber grafts. Real time force measurements will be taken every 6 hours over the 2-week experimental period.

Timeline (month of project): 14-15
Percent completion: 100%

Subtask 3: Set up 14-day bioreactor cultures of 3D bioprinted cellular and acellular collagen fibers using optimized conditions.

Timeline (month of project): 16-17
Percent completion: 75%

Subtask 4: Test cellular and acellular collagen fiber grafts in the bioreactor to determine the effects of cyclic tensioning on long term stability and differentiation potential. Cell number and morphology, metabolic activity, and toxicity, and gene expression will be assessed.

Timeline (month of project): 18-24
Percent completion: 20%

Objective 3: Determine *in vivo* performance of acellular and cell-decorated microfluidic-produced collagen fibers in a rat Achilles tendon-MTJ injury model.

Major Task 3: Biomanufacture cellularized and acellular implants to repair surgically-induced Achilles tendon-MTJ defects in rats and compare to controls.

Subtask 1: Label clinical grade human MCS's (RoosterBio) for tracking in the animal model and determination of bioprinted cells compared to intrinsic cells upon tissue explants.

Timeline (month of project): 9-12
Percent completion: 100%

Subtask 2: Manufacture sterile, 3D bioprinted crosslinked collagen fibers grafts with and without labeled clinical grade MSCs (RoosterBio) for implantation.

Timeline (month of project): 13
Percent completion: 25%

Subtask 3: Implant grafts into rat Achilles defect model: 154 animals including refinement and cull animals. Surgical plan: 3 timepoints: 2, 6 & 12 weeks. Surgical groups: Suture alone, Acellular microfluidic grafts, Cellular microfluidics grafts and Untreated.

Timeline (month of project): 14-16
Percent completion: 5%

Subtask 4: Live imaging for animals with labeled cellular microfluidic grafts at days 1, 3, 7, 14, 42 & 84 using the IVIS Spectrum detection system.

Timeline (month of project): 14-18
Percent completion: NA

Subtask 5: Explant analysis for all animals: A) Mechanical testing to assess repair strength, B) Histology to determine tissue quality in the repaired tendon, MTJ and muscle, and C) Immunohistochemistry to detect the long-term engraftment of the human MSCs into the xenotransplantation model.

Timeline (month of project): 16-24
Percent completion: 5%

What was accomplished under these goals?

1) *Major activities*

Designed, manufactured, and optimized a novel custom three-dimensional (3D) biomanufacturing platform deemed Assembled Cell-Decorated Collagen (AC-DC) bioprinting.

Quantitatively assessed cellular and mechanical properties of AC-DC implants with comparison to native tissue properties.

Optimized cyclic strain bioreactor culture protocols and began assessment of synthetic tissue development *in vitro*.

Began *in vivo* testing toward assessing the use of AC-DC implants to regenerate functional, native-like tissue in a rodent myotendinous junction (MTJ) defect model.

2) *Specific objectives*

Developed a novel additive manufacturing approach to produce cellularized implants consisting of dense, highly aligned, strong collagen microfibers. Specifically, collagen microfibers were robotically coated with cells and wrapped in parallel to form 3D grafts with designed geometries.

Utilizing fluorescent labeling and image analysis protocols, we quantified cell viability, orientation, and distribution throughout printed grafts. Uniaxial tensile testing was used to determine mechanical properties of grafts. We found that AC-DC grafts closely mimic key properties of native tissue.

Developed and optimized a custom bioreactor setup and cyclic strain protocol to stimulate the synthetic development of tissue *in vitro* for assessment of mechanical strength, cellular arrangement, and gene expression.

Subcutaneously implanted AC-DC grafts to determine optimal implant design for the MTJ defect model and harvested limbs for optimizing mechanical testing and determining baseline properties.

3) *Significant results*

1. Concept and design

We developed a novel additive biofabrication approach deemed Assembled Cell-Decorated Collagen (AC-DC) bioprinting to produce cellularized implants consisting of dense, highly aligned, strong collagen microfiber. Specifically, collagen microfiber is coated with a cell suspension and robotically wrapped around a rigid frame. In mimicking native ligament and tendon ultrastructure, this cell-coated fiber is wrapped in parallel next to and on top of itself to form rectangular macrostructures of designed width, length, and thickness. This results three-dimensional (3D) structures consisting of layers of densely packed parallel collagen fiber with cells seeded uniformly throughout. Grafts are cultured on custom rigid frames with varying geometries to maintain the macroscopic shape and orientation of the fiber before removal. The use of these grafts aims to promote regeneration and recovery of function in musculoskeletal tissue injuries including the myotendinous junction.

To enable AC-DC fabrication, a custom extrusion printhead (**Figure 1A**) was designed and mounted to a Folger Tech FT-5 R2 commercial 3D printer. Two separate planetary geared stepper motors with lead screw assemblies mechanically compress disposable syringes individually, extruding cell suspension with sub-microliter resolution. While a single cell suspension is printed at a time herein, the dual-solution printhead will prospectively facilitate the production of heterogeneous implants with differing cell populations in distinct regions.

During printing, cell suspension is extruded into the seeding manifold, where it builds up in a small coating reservoir (**Figure 1B**). Collagen microfiber was produced using a wetspinning process, desiccated, wound onto custom spools, and sterilized by electron beam sterilization prior to printing. Up to 3 spools of collagen microfiber are utilized during printing, each of which is fed through the seeding manifold. Within the seeding manifold, the collagen fiber is uniformly coated by the extruded cell suspension. The volume of cell suspension extruded per millimeter of drawn fiber is a user-determined process parameter and offers a means to control the resulting cell density and total number of cells throughout a graft.

A custom collection assembly was designed (**Figure 1A**) in which small rigid frames (**Figure 1C**) are held between two stepper motors. Typically, frame designs consist of two horizontal bars or dowels held a fixed distance apart by custom 3D-printed frame ends, forming a central opening to limit the effects of cell migration from the implant to the frame and additionally enable improved nutrient diffusion to the implant from surround cell culture media. A number of frame geometries have been utilized depending on the desired functional aspects, such as facilitating production of multiple implants or larger implants, securing loose fiber ends from the beginning and end of printed implants, or allowing straightforward handling and removal of implants from the frames. Stepper motors driving the frame rotation are mounted on manual linear stages which allow for straightforward loading and removal of frames between consecutive prints.

Prior to printing, fiber is fed through the seeding manifold and attached at an initial anchoring point on the collection assembly. As the frame is rotated by the motors, fiber is drawn under tension through the seeding manifold and coated by the extruded cell suspension. By coordinating the rotation of the frame and linear translation of the printhead along the width of the frame (the feed), cellularized implants of dense, highly aligned collagen microfiber are produced.

A custom Python code was developed to accept user inputs for designed implant geometry and printing parameters, number of implants per frame, implant width, height, number of layers of fiber, extruded volume of cell suspension per millimeter drawn fiber, feed distance between parallel fibers, and frame rotation rate, and output a corresponding g-code file. The g-code file contains all parameters and motion/extrusion commands to execute a designed print, and is sent to the printer to produce the designed implant.

To print cellularized implants, cells are suspended in a hyaluronic acid (HA) solution prepared in Dulbecco's Modified Eagles Medium (DMEM) or a cell-type specific culture media. Hyaluronic acid is a key component of the extracellular matrix and is utilized herein as a "cellular glue" to facilitate the adherence of cells to collagen microfiber. Culture media provides the necessary nutrients and cytocompatible environment to sustain cell health during printing.

Printing process parameters were optimized to facilitate consistent and controlled fabrication. HA concentrations ranging from 2.5 mg/mL to 10 mg/mL were tested for handleability and printability. It was found that an optimal concentration of 5 mg/mL could be accurately pipetted and extruded, readily filtered using a 0.2 um filter for sterilization, provided sufficient viscosity to limit cell settling during printing, and facilitated uniform coating of collagen fiber with cell suspensions. An extrusion rate of 0.38 µL per 10 mm of drawn fiber was found to result in uniform coating of fiber. A feed distance between adjacent fiber strands of 0.15 mm was found to be optimal and could be varied to control implant porosity. A frame rotation rate of 10 rpm was used to produce implants quickly and did not appear to affect cell health due to fluid shear stresses.

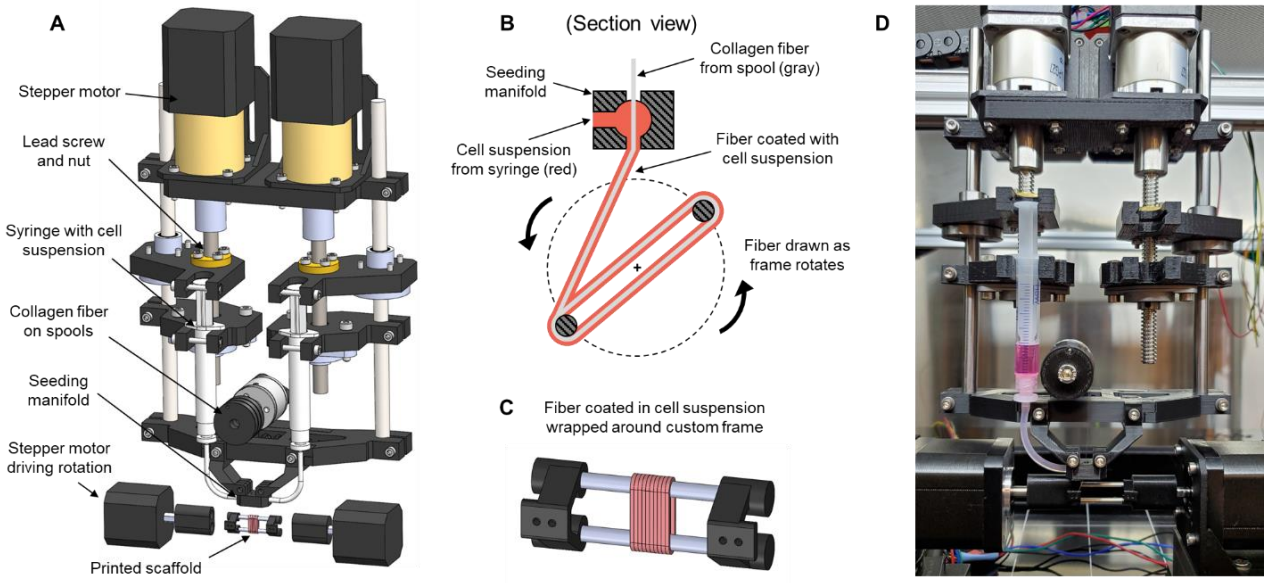

Figure 1. Cell-decorated collagen fabrication system design. (A) CAD model of custom extrusion printhead and frame assembly with key components identified. (B) Section view illustrating the cell seeding and implant biofabrication process. Collagen fiber passes through a seeding manifold, where it is uniformly coated with a cell suspension. The coated fiber is drawn onto a frame of arbitrary shape and dimensions and wrapped in parallel and on top of itself to form an implant. (C) Enlarged CAD model of parallel fiber implant wrapped around a rigid frame with a multifunctional design. (D) Photograph of printhead and frame assembly during printing.

2. Assessment of bioprinting fidelity

Cellularized collagen microfiber implants were printed rapidly and repeatably onto various frame geometries (**Figure 2A, B, C**). Multiple implants were printed onto frames consisting of two steel dowels held together by 3D-printed PLA frame ends and secured into individual bundles by tying knots at each end using suture (**Figure 2A**). Custom PLA frames were used to print larger implants (**Figure 2B**) and frame geometries can be easily modified for producing millimeter to centimeter scale implants. Specialized frame geometries were used to print implants directly onto and between two lengths of suture and maintain tension on implants during culture (**Figure 2C**). After securing implants into bundles using suture, they can be easily removed from the frames (**Figure 2D**) by removing one or both PLA frame ends and sliding implants off of the steel dowels, for example. Regardless of custom geometry, rigid frames were found to maintain fiber alignment and macrostructure of printed implants in culture over several weeks.

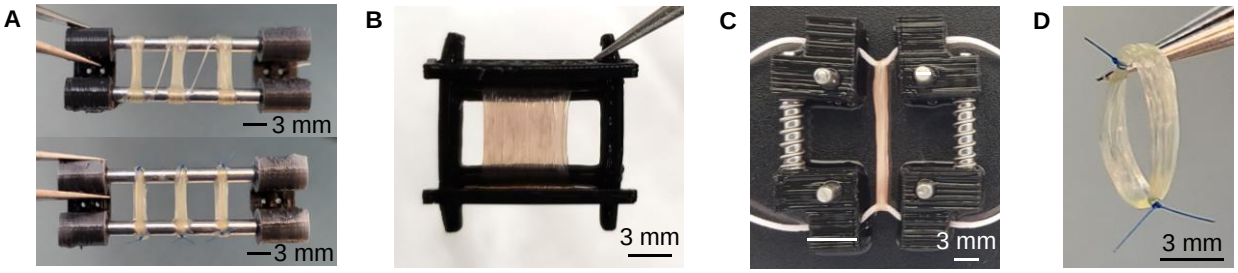

Figure 2. Printed test implants with varying implant and frame geometries. (A) Three printed implants on a multifunctional frame before (top) and after (bottom) being secured with suture. (B) A larger printed implant on another custom frame geometry. (C) An implant printed onto two lengths of suture and held in tension by a custom frame. (D) A printed implant held by tweezers after being secured with suture and removed from a frame.

Transmitted light microscopy of printed implants shows striations indicative of densely packed parallel fiber after 4 days of culture (**Figure 3A**). Fluorescence imaging of hMSCs stained with the cytoplasmic label DiD (green), dead cell nuclear label EthD-1 (red), and fiber autofluorescence at 405 nm (blue) shows implants after 4 days of culture with cells distributed throughout the implant (**Figure 3B**). Notably, cells are elongated parallel to the fiber direction as is typical for native tendon and ligament tissue. Images such as this were taken throughout varying fields of view and in different planes throughout implants as a qualitative means to assess cell distributions. Immediately after printing, cells were observed to have a largely uniform distribution throughout implants, with no observable localizations of comparatively high or low density. Similarly, cells maintained a largely uniform distribution during culture as they proliferated and eventually became confluent throughout printed implants. Cell suspensions ranging from 1×10^6 to 6×10^6 cells/mL were successfully printed, with optimal concentrations chosen based on the desired resulting graft cell density.

As a means to assess the fundamental consistency of the printing process, a single grouping of three collagen microfiber strands (printed simultaneously from 3 spools of fiber attached to the printhead) was printed with hMSCs and cells were labeled with the same fluorescent stains after 4 days of culture (**Figure 3C**). These three fiber strands act as the "building blocks" of printed implants, as three fiber strands are continuously drawn through the printhead, seeded with cells, and wrapped next to and on top of one another to form 3D implants. The uniformity of cells on these three "building block" strands is indicative of a consistent fundamental cell seeding process, such that resulting implants are expected to have consistent cellularity throughout, regardless of overall implant dimensions or geometry.

Cell viability throughout printed implants was assessed both qualitatively and quantitatively by fluorescent imaging of hMSCs stained with the cytoplasmic label DiD and dead cell nuclear label EthD-1. Qualitatively, a generally high viability is indicated by live cells (green) greatly outnumbering dead cells (red) (**Figure 3B, C**). Quantitatively, ImageJ was used with established particle counting approaches to compare the number of live and dead cells throughout implants immediately after printing. Across various implant geometries and printing conditions, cell viability was found to remain consistently above 80%. For representative grafts printed with typical process parameters, hMSCs were found to be 93.2±1.7% (standard deviation, n=6) viable immediately after printing. Over extended culture periods, quantifying cell viability by fluorescent imaging becomes difficult as cells become confluent throughout the implants with individual cells becoming essentially indistinguishable (**Figure 4A**). Qualitatively, it was observed that cells maintain a very high viability during extended periods of culture, with live cell numbers estimated to be in the tens of thousands greatly outnumbering dead cells.

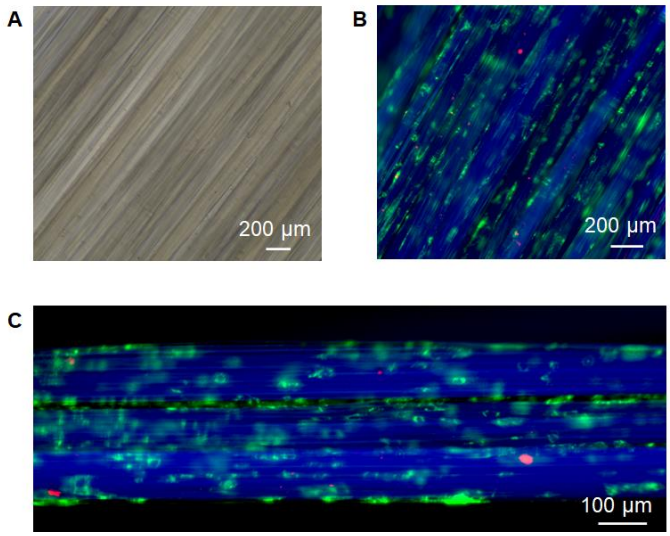

Figure 3. Microscopic imaging of printed implants. Fluorescence images show all cells with the cytoplasmic label DiD (green), dead cell nuclei label EthD-1 (red), and collagen fiber autofluorescence at 405 nm (blue). (A) Transmitted light image of a printed implant showing striations indicative of densely packed parallel fiber after 4 days of culture. (B) Fluorescence image showing hMSCs uniformly distributed throughout and elongated parallel to the fiber direction after 4 days of culture. (C) Fluorescence image showing hMSCs attached to and distributed along three strands of collagen fiber after 4 days in culture.

Benchmark implants were printed with hMSCs suspended at 4×10^6 cells/mL to assess cell metabolic activity over time using the alamarBlue assay. Implants (n=6) were incubated for 6 hours in 10% alamarBlue solution in hMSC growth media and fluorescence was measured after 1, 4, and 7 days in culture according to standard assay protocols (**Figure 4B**). Metabolic activity of cellularized implants in culture was found to increase 5-fold over 7 days of culture, indicating an increase in cell health, activity, and proliferation.

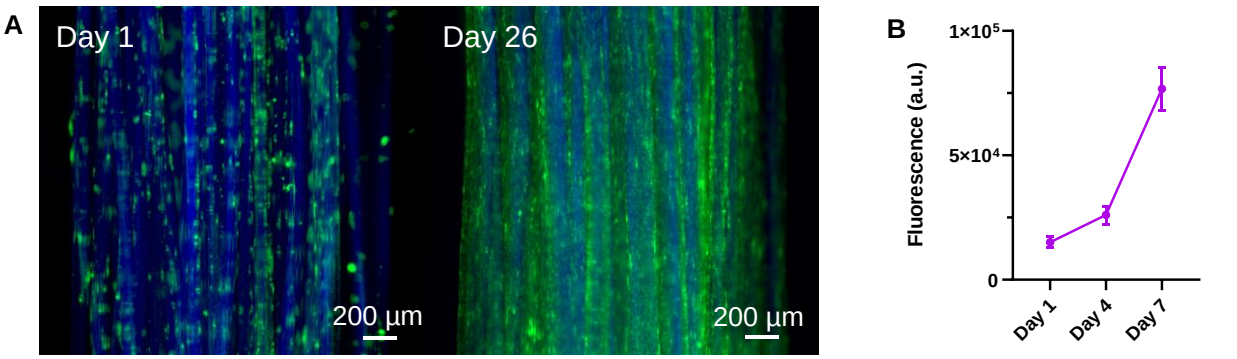

Figure 4. Cell proliferation and metabolic activity. Fluorescence images show all cells with the cytoplasmic label DiD (green) and collagen fiber autofluorescence at 405 nm (blue). (A) Fluorescence images of printed implants showing a largely uniform initial distribution of cells after 1 day of culture and a confluent densely-cellularized implant after 26 days of culture. (B) Fluorescence indicating an increase in cell metabolic activity using the alamarBlue assay for implants printed with human tenocytes after 1, 3, and 7 days of culture. Error bars represent standard error of measurement.

3. Assessment of cellular distribution and uniformity

The uniformity of cells distributed throughout implants was quantified by adapting a method for analyzing the distribution of particles in a field of view using Shannon entropy. This approach offers a means to validate the bioprinting process control and repeatability, and may be applied to various tissue engineering approaches which have traditionally relied on subjective and qualitative descriptions. In a typical 2 mm × 2 mm field of view of a printed implant, rat muscle progenitor cells (rMPCs) were stained and imaged with the cytoplasmic label DiD (green) after 14 days in culture with fiber autofluorescence at 405 nm (blue) (**Figure 5A**). The image was converted to binary, such that cells are shown in black on a white background (**Figure 5D**). Image analysis was then used to measure the average grayscale value, with white pixels measured as 0 and black pixels measured as 255, of pixel columns taken across the 2 mm transverse direction, with the value for each column being the average grayscale value of pixels contained in that column. Similarly, the grayscale value is measured for pixel rows taken along the longitudinal direction with the value for each row being the average grayscale value of pixels contained in that row. These measured grayscale values were then grouped into 100 bins and normalized to the total grayscale value of the field of view to represent the relative cellularity. This relative cellularity is plotted across the transverse (**Figure 5E**) and longitudinal (**Figure 5F**) directions.

Plotting the relative cellularity measured across the transverse or longitudinal directions of an implant offers a means to visualize the local number of cells, corresponding to the number of black pixels, throughout (**Figures 5E, F**). Variations in these values represent local variations in the number of cells present. Linear regression analysis is used to fit a straight line to the grayscale distributions as a means to represent the uniformity across the field of view. For a perfectly uniform distribution, linear regression will result in a horizontal line. It's seen that linear regression results in a nearly horizontal line when measured across both the transverse and longitudinal directions (**Figure 5E, F**), indicating a largely uniform distribution of cells throughout the field of view.

The distribution of cells throughout a field of view can also be quantified using particle analysis methods. The uniformity measure U (**Equation 1**) is defined using the Shannon entropy of the printed implant, $s_{printed}$, Shannon entropy of a perfectly nonuniform particle distribution, $s_{nonuniform}$, and Shannon entropy of a perfectly uniform particle distribution, $s_{uniform}$. Shannon entropy s (**Equation 2**) is calculated for a field of view with N pixel columns/rows across a field of view based on the probability p_j (**Equation 3**) that a particle lies within the jth pixel column/row, where m_j is the grayscale value of the jth column/row and M is the sum of grayscale values across the field of view. The uniformity value U ranges from 0 for a perfectly nonuniform distribution in which cells are present in exactly half of the field of view, to 1 where cells are present exactly equally throughout the full field.

$$U \equiv \frac{s_{printed} - s_{nonuniform}}{s_{uniform} - s_{nonuniform}} \qquad \textbf{Equation 1}$$

$$s = -\sum_j^N p_j \ln p_j \qquad \textbf{Equation 2}$$

$$p_j = \frac{m_j}{M} \qquad \textbf{Equation 3}$$

For the typical field of view shown in **Figure 5A**, uniformity measured across the transverse direction U_{trans} is 0.87, indicating a largely uniform distribution of cells. Uniformity measured across the longitudinal direction U_{long} is 0.95, indicating a distribution even closer to perfectly uniform. Reasoning for the variation in these measures can be visualized in **Figure 5E** and **Figure 5F**. More severe peaks and valleys are present in relative cellularity values measured across the transverse direction when compared to those measured across the longitudinal direction. This can be attributed to cell elongation, which acts to increase the grayscale value in the direction of elongation (pixel columns measured across the transverse direction). Regardless, both measures are indicative of a high uniformity of cells throughout the field of view. Across multiple printed implants with varying cell types and in multiple fields of view, the measured uniformity U was greater than 0.8, indicating that AC-DC fabrication consistently produces uniformly cellularized implants.

The alignment of cells within implants was also quantified for typical implant printed with human tenocytes stained and imaged with the cytoplasmic label DiD (green) after 4 days in culture. Directionality analysis of the fiber-only component of using fiber autofluorescence at 405 nm with the peak normalized to 0 degrees shows a narrow frequency distribution, indicating highly parallel fiber with nearly all directional components within 10 degrees of the peak orientation (**Figure 5B**). Similarly, directionality analysis of the cell-only component of the implant shows a frequency distribution with a peak orientation identical to the fiber direction, indicating a significant degree of cell alignment and elongation in the direction of the fiber (**Figure 5C**). Across multiple printed implants with varying cell types and in multiple fields of view, a high degree of directionality was measured for fiber and cells, indicating that cells align with the highly parallel fiber.

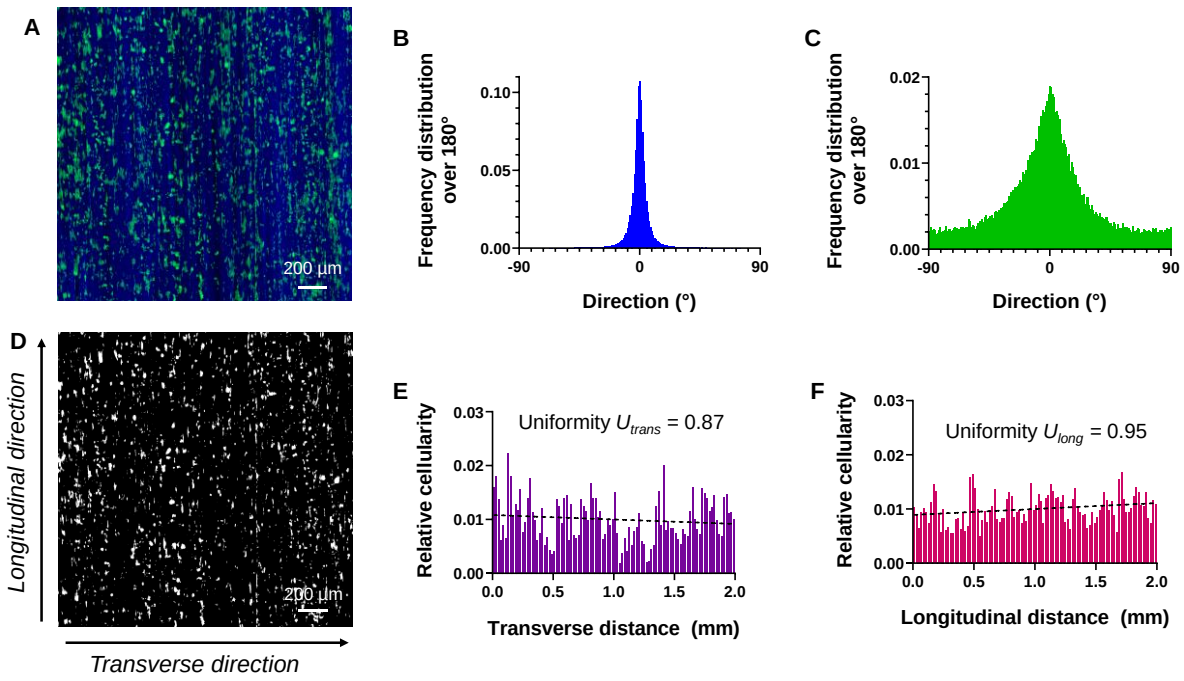

Figure 5. Quantitative cell distribution and alignment. (A) Typical field of view of a printed implant with rat muscle progenitor cells distributed throughout and aligned after 14 days in culture. Fluorescence image shows all cells with the cytoplasmic label DiD (green) and collagen fiber autofluorescence at 405 nm (blue). (B) Directionality analysis of the fiber-only component of a typical printed graft, indicating highly parallel fiber. (C) Directionality analysis of the cell-only component of a typical printed graft, indicating a high degree of alignment in the fiber direction. (D) Image shown in A converted to binary for cell distribution analysis with cells indicated in white, background in black, and transverse and longitudinal directions labeled. Relative cellularity plotted along the transverse (E) and longitudinal (F) directions, with nearly horizontal linear regression (dashed lines) and quantified uniformity measure U (ranging from 0 to 1) indicating a highly uniform distribution of cells.

4. Assessment of graft mechanical properties

Collagen microfiber implants were printed with and without cells using the AC-DC fabrication approach and their mechanical properties were assessed. Cellular implants were printed with hMSCs and acellular implants were produced using identical conditions. Implants were tested after 1 day and 28 days in culture and imaged after 1 day and 26 days in culture (**Figure 4A**), closely corresponding to the mechanical testing timepoints. Implants were secured using suture at each end, removed from frames, and returned to culture media the day of testing for implants tested after 1 day of culture and the day prior to testing for implants tested after 28 days of culture.

Implants were mounted to a custom 2-pin setup (**Figure 6A**) on a uniaxial tensile testing machine (MTS Systems Corporation, Eden Prairie, MN) with a 100 N load cell. The 2-pin setup allows for implants secured with suture to be looped around two horizontal steel dowel pins, each of which is mounted to the tensile testing machine such that the distance between the pins increases during testing. This approach was found to provide significantly more consistent results when compared to mounting implants in standard compression grips, which often lead to implant damage, slippage, or staggered breakage of individual fibers within an implant. Implants were pulled to failure with a pin displacement speed of 1 mm/sec and load and displacement data were recorded. Ultimate tensile stress (UTS) was determined by the peak load and implant cross sectional area, and tangent modulus was determined by the slope of the linear region of the stress-strain curve. Strain at break was determined by the initial gauge length and pin displacement at failure. Typical stress-strain curves for each tested group are shown in **Figure 6B**, with distinct "toe" regions of gradually increasing slope followed by linear regions of maximum slope and ultimately sharp well-defined decreases in stress at failure.

Mechanical properties were calculated and reported using two methods for determining the cross-sectional area of printed implants. First, the "solid only" cross-sectional area was determined by multiplying the measured cross-sectional area of individual collagen fibers by the total number of constituent fibers within the printed grafts. The diameter of individual hydrated fibers was measured using microscopic imaging, and the total number of constituent fibers was a controlled user input to the printing process. Second, the "full graft" cross-sectional area was measured manually using digital calipers. Comparing these two methods, mechanical properties determined using the solid only cross section are indicative of the properties of the constituent collagen fiber comprising the grafts, while properties determined using the full graft cross section consider the void space and inherently limited packing density of constituent fiber. Solid only cross-sectional area was assumed to be identical for each experimental group based on the stability of the constituent collagen fiber in culture, and full graft cross-sections were measured for each experimental group immediately prior to testing (**Figure 6C**).

UTS, tangent modulus, and strain at break, are shown in **Figure 6D, E, and F**, respectively, for acellular and cellular implants tested to failure after 1 day and 28 days of culture (n=10 for all groups). For plots displaying UTS (**Figure 6D**) and tangent modulus (**Figure 6E**), horizontal lines are plotted representing the mean UTS and tensile modulus of human ACL (*a)* [Appendix A, journal article], of the strongest portion of the human supraspinatus tendon (*b)* [Appendix B, journal article], and of typical collagen gels used in tissue engineering (*c)* [Appendix C, journal article]. It's seen that depending on the method for determining cross-sectional area, both acellular and cellular implants produced using AC-DC fabrication nearly match or exceed key mechanical properties of representative native human tendons directly after printing and continue to do so after 28 days in culture. Additionally, the UTS and modulus of collagen microfiber implants produced using AC-DC fabrication are orders of magnitude larger than the strength and stiffness of collagen gels commonplace in biomanufacturing approaches, which have a typical UTS on the order of 20 kPa and typical tensile modulus on the order of 200 kPa [Appendix C, journal article]. Both acellular and cellular implants after 1 day and 28 days in culture had mean failure strains ranging from 20% to 25% (**Figure 6F**). Unlike UTS and modulus, strain is not dependent on cross-sectional area such that results do not differ when the considering solid only or full graft measurement approaches.

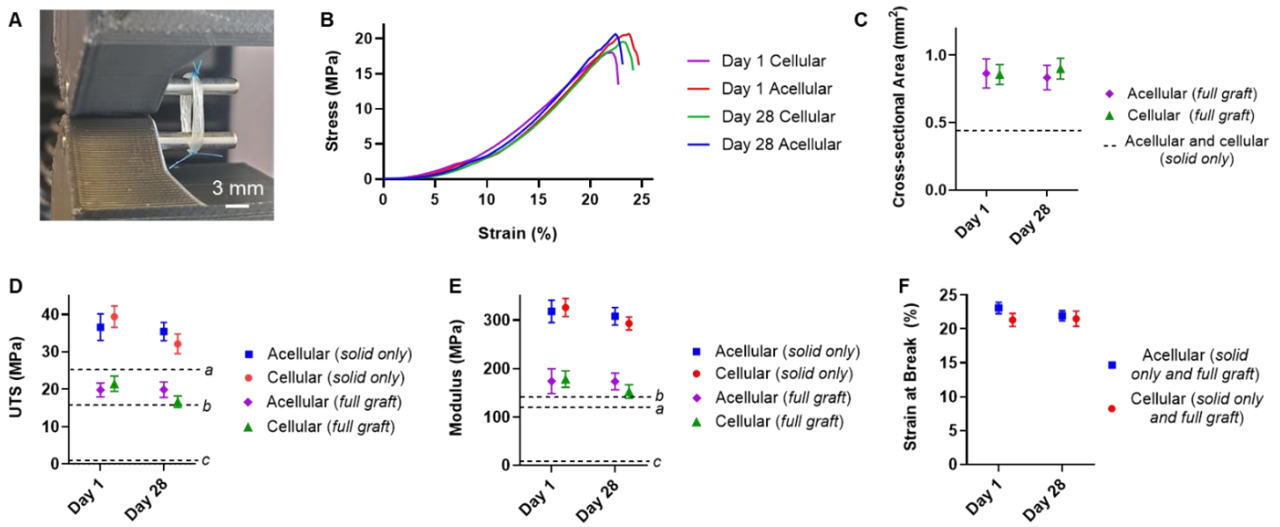

Figure 6. Implant mechanical properties. Data obtained from acellular implants (n=10 each time point) and cellular implants (n=10 each time point) containing hMSCs after 1 day and 28 days of culture. Error bars represent standard deviation. (A) 2-pin uniaxial tensile tensing setup offering improved consistency compared to traditional compression grips. (B) Typical stress-strain curves for each experimental group based on the "full graft" with cross-sectional area. (C) Measured full graft and solid only cross-sectional areas. (D) Ultimate tensile stress (UTS). (E) Tangent modulus. (F) Strain at break. [a] Mean UTS and modulus of human ACL [Appendix A, journal article]. [b] Mean UTS and modulus of the strongest portion of the human supraspinatus tendon [Appendix B, journal article]. [c] Mean UTS and modulus of typical collagen gels used in tissue engineering [Appendix C, journal article].

In all, using clinically relevant biomaterials and cells, the novel AC-DC biofabrication process is capable of printing constructs mimicking some of the biological, morphological, material, and functional properties of native musculoskeletal tissue. Graft geometries are customizable and well-controlled. Cells are found to maintain high viability, proliferate, and elongate with uniform cellular distributions throughout grafts. Graft mechanical properties are found to mimic those of native tissue and exceed the properties achieved by traditional tissue engineering approaches by orders of magnitude.

5. Optimization of cyclic strain bioreactor culture protocols

Utilizing AC-DC bioprinting, we produced acellular and cellular collagen fiber grafts to study synthetic tissue development during bioreactor culture. Grafts of 9 mm length and 1 mm width consisting of 4 layers of collagen fibers were produced. These dimensions match those of grafts which will be utilized in upcoming animal studies to repair the rat Achilles myotendinous junction. Cellular grafts were printed utilizing previously optimized parameters, with 4×10^6 cells/mL suspended in a 5 mg/mL hyaluronic acid (HA) solution. Acellular grafts were printed with only a 5 mg/mL HA solution. hMSCs were utilized for all experiments due to their well-established therapeutic effects and availability as a quality-controlled clinically relevant resource. Fluorescence microscopy was used to confirm printed graft consistency.

Custom bioreactor hardware components were designed and implemented to facilitate bioreactor testing of our collagen fiber implants. We found that traditional compression grips lead to fiber damage, slippage, and nonuniform strain across grafts under tension. To address this, we designed pin-based fixtures similar to our previously utilized setup for uniaxial tensile testing to incorporate with our bioreactor hardware (**Figure 7**). Top and bottom fixtures with 6 stainless steel pins each were affixed to the top and bottom grips inside the bioreactor chamber, respectively. The displacement of the top grip is controlled, such that six AC-DC grafts can be loaded and cyclically tensioned within the chamber at a time. The setup was found to enable uniform distribution of strain across samples while mitigating graft damage. Additional components including a redesigned external clamp to immobilize the top mounting fixture during graft loading/unloading and retention plates to prevent graft slippage off of the pins were also designed. All components were 3D printed from PLA, which has been shown to remain stable and inert during extended periods of culture.

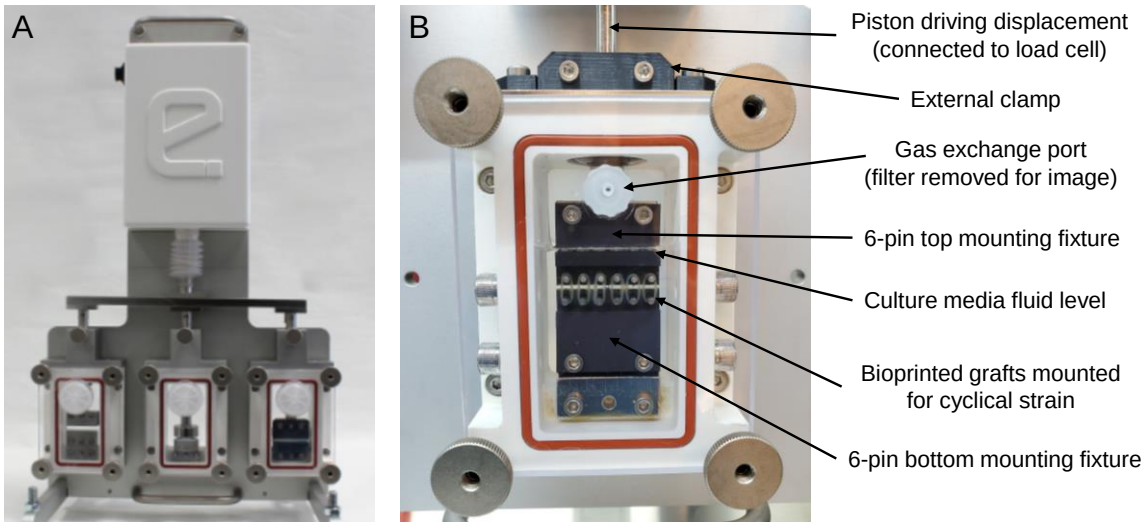

Figure 7. Bioreactor system and key components. (A) Stock EBERS TC-3F cyclical strain bioreactor system with real-time force monitoring capabilities. (B) Individual bioreactor chamber with custom hardware components loaded with six bioprinted collagen fiber implants.

With updated hardware, we tested varying cyclic displacement patterns, strain amplitudes, and handling methods to develop an optimized bioreactor protocol. Based on review of relevant literature and our bioreactor capabilities, we determined that velocity-driven triangle or trapezoid waves would be most appropriate for inducing cyclic strain (**Figure 8**). The top grip is mounted to 50 N load cell, enabling continuous force monitoring during testing. Grip velocity was set to 0.1 mm/s and grips travel to the prescribed maximal displacement, hold for a prescribed dwell time, return to the initial position, and hold again for a prescribed dwell time. We investigated dwell times of 0 (**Figure 8A**), 1.4 s (**Figure 8B**), and 10 s (**Figure 8C**). Gradual changes in force readings were observed during dwell times which likely indicates stress relaxation of the grafts. While including a dwell time in the protocol would enable additional mechanical property characterization based on this stress relaxation, it significantly limits the number of cycles which can be completed per hour. The number of cycles has been shown to strongly affect strain-induced tissue development, which is our primary concern, such that we chose to omit any dwell time and use a simple triangle wave in continuing studies. Regardless of strain protocol, we found that acellular and cellular grafts behaved essentially identically.

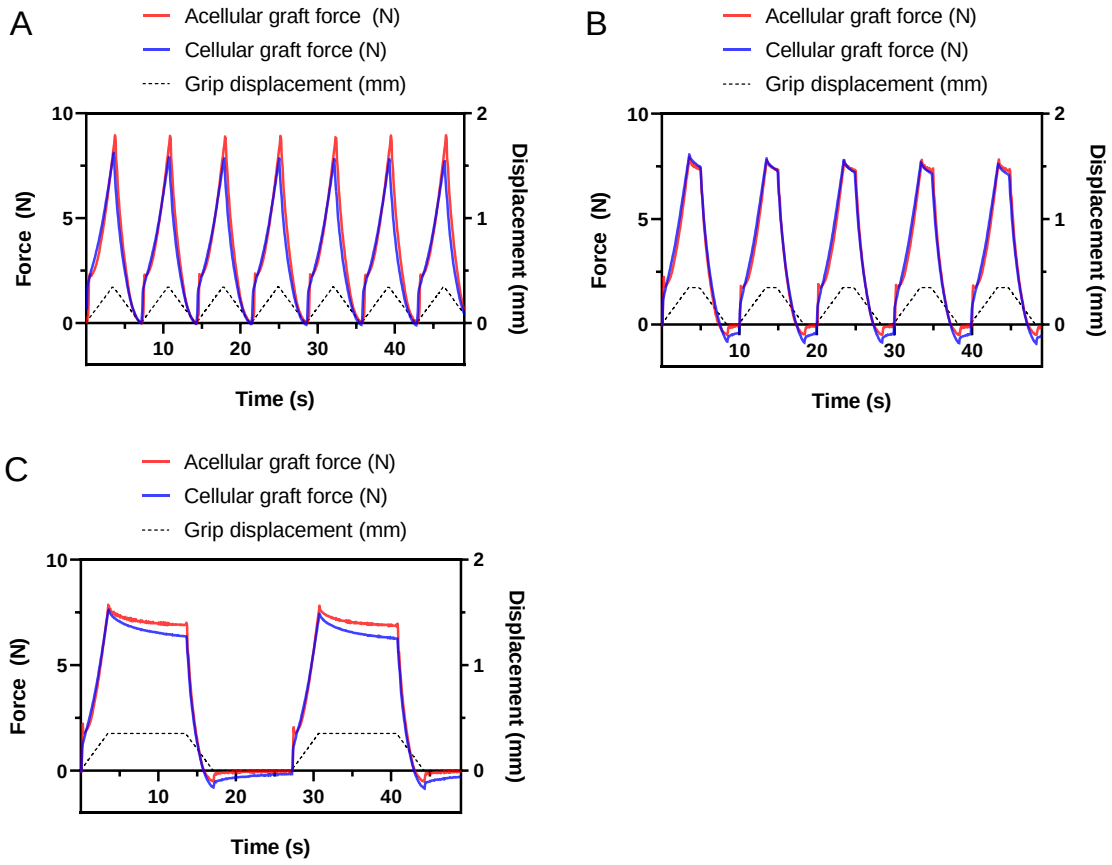

Figure 8. Real-time force measurements for acellular and cellular grafts undergoing varying cyclic strain protocols. Force is plotted on the left vertical axis and displacement is plotted on the right vertical axis. (A) Triangle wave displacement with no dwell time. (B) Trapezoid wave displacement with 1.4 s dwell time. (C) Trapezoid wave displacement with 10 s dwell time.

Based on review of relevant literature, strain amplitudes between 2.5% and 5% were investigated to facilitate optimal synthetic tissue development. We theorized that 5% strain may induce a more significant cellular response than 2.5%. During this initial testing, graft stiffness was determined in real time based on the change in measured force, prescribed grip displacement (strain), and graft cross sectional area. For comparison, we plot normalized stiffness as a percent of initial stiffness measured for each experimental group.

We found that 5% strain led to a significant decrease in both acellular and cellular graft stiffness over the first 72 hours of testing (**Figure 9A**). Acellular grafts experienced a gradual decrease to ~40% of their initial stiffness, while cellular grafts experienced a very rapid decrease to ~20% of their initial stiffness. We theorize that this is due to the slippage of adjacent collagen fibers within each graft. Prior to bioreactor testing, AC-DC grafts are removed from temporary frames and affixed into circular bundles using suture. These bundles rely on friction between adjacent fibers to resist tensile forces which would otherwise cause unraveling. Thus, the perceived decrease in stiffness when undergoing 5% strain is likely attributed to grafts gradually unraveling and increasing in length, leading to a decrease in measured force. This effect is more pronounced for cellular grafts, for which cells and their deposited ECM act as a lubricant between fibers and reduce friction resistance.

However, we found that this unraveling and perceived decrease in stiffness was not significant at 2.5% strain (**Figure 9A**). Cellular grafts undergoing 2.5% strain experienced only a minor rapid drop to ~90% of their initial stiffness, then remained stable for 72 hours. Based on these results, we will utilize 2.5% strain in continuing studies to ensure consistent strain application during bioreactor culture. Additionally, based on review of literature we have chosen to implement a 50% ON 50% OFF strain cycle, where grafts undergo cyclic stain for 3 hours, followed by a 3-hour rest period, alternating between the two for study durations up to 14 days. These parameters in conjunction with our choice of cyclic triangle wave displacement complete our bioreactor protocol optimization.

We conducted a 14-day test run using optimized conditions with cellular AC-DC grafts. Cellularized grafts which had previously been grown in static culture were used to confirm that cells remained viable during bioreactor culture. The alamarBlue assay for cell metabolic activity was utilized with standard protocol at day 0 before being loaded into the bioreactor and cultured under cyclic strain. At days 7 and 14, the strain protocol was paused, grafts were removed from the bioreactor chamber, and the alamarBlue assay was conducted. Samples were returned to the bioreactor chamber and the protocol was resumed at each time point. This confirmed our ability to pause the process, aseptically handle and measure graft properties, and continue culture for future experiments using nondestructive testing for graft analysis. Fluorescence intensity measured using the assay indicates that cells remained viable and metabolically active over the 14-day culture period, with no statistically significant change (**Figure 9B**). It is important to note that cellularized grafts which had previously reached confluency in static culture were utilized in this test run to confirm cell survival. In future experiments, freshly printed grafts will be utilized, for which we will expect to see an increase in metabolic activity as cells within grafts proliferate over time.

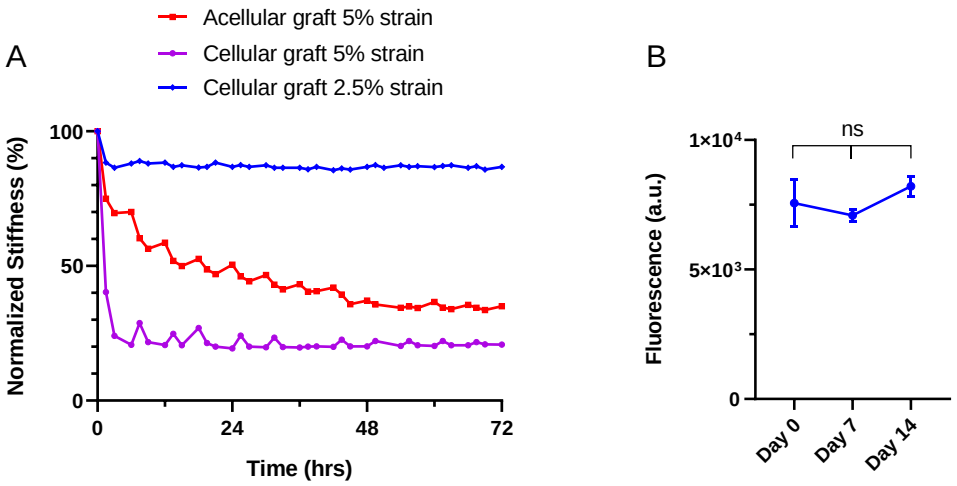

Figure 9. (A) Measured stiffness over 72 hours of cyclic strain for bioprinted grafts shown as a percent of initial stiffness. Acellular and cellular grafts experienced decreases in stiffness at 5% strain, while cellular graft stiffness remained constant at 2.5% stain. (B) Fluorescence measured using the alamarBlue assay for cell metabolic activity, indicating that cellular grafts remained viable over 14 days of optimized bioreactor culture (n=3).

6. Further bioprinting process optimization

In preparation for the rat Achilles myotendinous junction repair model, we tested cell labeling approaches to facilitate *in vivo* cell tracking. The ability to image and track implanted cells over time offers valuable insight into cell residency, proliferation, and the therapeutic effects of implanted vs. intrinsic cells. Luciferase is a light-emitting enzyme responsible for the bioluminescence of fireflies, and can be utilized to track cells *in vivo*. We attempted to edit the genome of hMSCs to express luciferase using commercially available CRISPR products. However, we encountered challenges limiting the feasibility of the approach. Stem cells have historically been difficult to transfect, and we unfortunately observed a very low transfection efficiency in treated cells to where luminescence was not detectable. We explored commercial options from companies producing custom cell lines, but luciferase transfection for hMSCs was outside of their capabilities. As such, we will proceed with alternative labeling approaches including the fluorescent markers DiD and DiI to facilitate cell tracking *in vivo*. We have previously confirmed the effectiveness of these fluorescent stains *in vitro* and their successful use *in vivo* has been reported. For the upcoming rodent myotendinous junction (MTJ) repair model, these fluorescent labels in conjunction with human-specific immunostaining will allow us to track the long-term engraftment of implanted cells and distinguish them from infiltrating native cells, as originally proposed.

With animal work delayed by mandatory facility closures due to COVID-19, we conducted supplemental studies aiming to further develop our biofabrication capabilities and improve the outcomes of upcoming tasks. These additional studies closely align with our proposed project goals and include 1) Use of fibrin gel as a matrix material and 2) Cryopreservation of bioprinted grafts.

As detailed in previous reports, our novel Assembled Cell-Decorated Collagen (AC-DC) biofabrication process has utilized a hyaluronic acid (HA) solution as a matrix material and binder to facilitate the attachment of cells to collagen microfiber grafts. While characterization of our bioprinted grafts has shown that HA facilitates cell attachment and has low cytotoxicity *in vitro*, literature suggests that in some cases HA may cause adverse inflammatory responses *in vivo*.

As such, we have investigated the use of fibrin as a bioprinted matrix material as a possible alternative to HA. Fibrin is a naturally occurring protein formed during the clotting of blood, has been widely used in FDA-approved medical procedures, and offers promise as a tissue engineering material due to its biocompatibility, bioactivity, and mechanical properties. Whereas hMSCs were suspended in an HA solution previously, they were instead suspended in a 40 mg/mL bovine-derived fibrinogen solution (2×10^6 cells/mL). As before, the AC-DC bioprinting process was used to controllably coat collagen microfiber with this cell suspension as the fiber was wrapped next to and on top of itself to form 3D grafts with cells distributed throughout. During printing, grafts were hydrated with a 0.452 mg/mL bovine-derived thrombin solution, which initiated the rapid solidification of the fibrinogen cell suspension and formation of a stable fibrin gel.

Microscopic imaging revealed that fibrin is suitable for use as an AC-DC bioprinting matrix. Transmitted light shows high geometric fidelity grafts comprised of densely packed parallel collagen fiber (**Figure 10A**). Fluorescence imaging with DiD (green) and fiber autofluorescence (blue) shows grafts with hMSCs distributed throughout after 7 days in culture (**Figure 10B**) and confluent densely-cellularized grafts after 21 days in culture (**Figure 10C**). Future studies will further investigate both fibrin and HA as materials for use with AC-DC bioprinting with a transition to one approach if it is found to be superior.

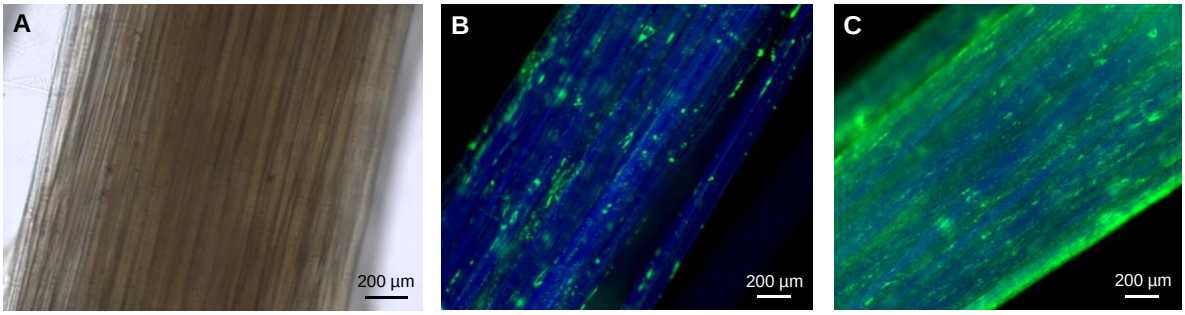

Figure 10. Microscopic imaging of AC-DC grafts printed using fibrin as a matrix material. (A) Transmitted light image after 1 day in culture showing parallel collagen microfiber. (B) Fluorescent images after 7 days in culture and (C) after 21 days in culture showing cells (hMSCs) with the cytoplasmic label DiD (green) and collagen fiber autofluorescence at 405 nm (blue).

The cryopreservation of cellularized bioprinted grafts was also investigated to improve the logistics linking graft production, transportation, and surgical delivery. In this pilot study, cellularized grafts printed with both HA and fibrin as matrix materials were produced, cryopreserved using the commercial cryopreservative CryoSOfree, and thawed after 7 days of storage in liquid nitrogen. Cellularized grafts were produced with hMSCs using typical materials and process parameters, as described above and in previous reports. Cryopreservation, thawing, and subsequent culture were done according to recommended standard protocols.

Cell metabolic activity (hMSCs) was quantified using the alamarBlue assay for grafts printed with HA and with fibrin (n=3 each) prior to cryopreservation and at 0, 1, 4, and 7 days after thawing (**Figure 11A**). Metabolic activity prior to cryopreservation acts as a baseline for comparison, and subsequent relative fluorescence measurements act as a means to assess both the cytocompatibility of the freeze-thaw process and recovery of the cellularized grafts in culture. A decrease in cell metabolic activity was observed for both HA and fibrin samples when measured immediately after thawing as well as 24 hours after thawing, indicating a possible latent effect of the cryopreservation process on cell viability and activity. While cell metabolic activity was found to increase for samples printed with an HA matrix from day 1 to day 7, activity remained stagnant for samples printed with fibrin during this period. This indicates that cell health and activity more easily recovers using HA as a matrix, and could potentially be due to microarchitectural changes induced in the fibrin gel during the freeze-thaw process. In all, results from this pilot study are encouraging and warrant further investigation including alternative cryopreservation materials/protocols.

The mechanical properties of cellularized grafts were investigated before and after cryopreservation to assess the effects of the freeze-thaw process on collagen fiber strength/stiffness. While fibrin was used as the matrix material, neither HA nor fibrin are expected to contribute significantly to the mechanical properties of printed grafts as the properties of these matrices are orders of magnitude below those of the collagen fiber. Uniaxial tensile testing was conducted with standard protocols detailed in previous reports to test grafts to failure. Graft ultimate tensile strength (UTS) (**Figure 11B**) and tangent modulus or stiffness (**Figure 11C**) were determined before and after cryopreservation (n=3 each). In this pilot study we did not observe a statistically significant difference in either strength or stiffness due to cryopreservation, indicating that the freeze-thaw process does not appreciably affect the mechanical properties of AC-DC collagen fiber grafts.

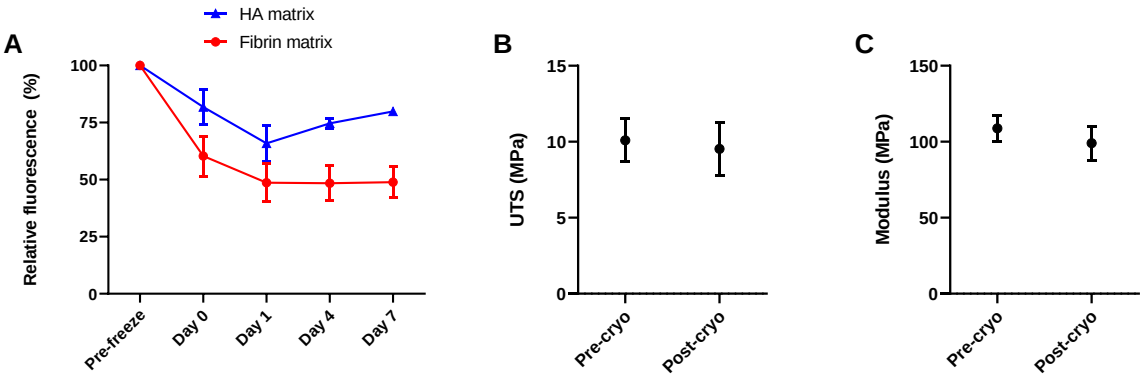

Figure 11. Metabolic activity and mechanical properties of AC-DC grafts before and after cryopreservation. (A) Fluorescence intensity relative to pre-freeze values measured using the alamarBlue assay indicating cell metabolic activity for HA and fibrin grafts printed with hMSCs. (B) Ultimate tensile strength and (C) tangent modulus of fibrin grafts printed with hMSCs. Error bars indicate standard deviation.

We developed an improved fibrin-based 3D bioprinting approach (**Figure 12A**) following the initial promising results of utilizing fibrin as a printed matrix material discussed in the previous report. Using the new approach, hMSCs are suspended at 4×10^6 cells/mL in a printing solution of 40 mg/mL bovine-derived fibrinogen prepared in hMSC media. This printing solution is then controllably extruded by our custom printhead to coat strands of collagen fiber as both the fibrinogen solution and fiber pass through a seeding manifold and dispensing tip. As with our previous printing processes, cell-coated fiber is wrapped onto a robotically controlled rotating temporary frame to form 3D grafts of designed geometries.

While graft formation was previously conducted in air, our current approach implements a bath of 7 U/mL bovine-derived thrombin solution prepared in hMSC media in which grafts remain submerged during printing. A custom rotation assembly was designed (**Figure 12B**) to facilitate submerged printing. As collagen fiber coated with the extruded fibrinogen cell suspension contacts the bath, the thrombin rapidly initiates the solidification of the fibrinogen and formation of a stable fibrin gel. This process binds cells to the fiber and was found to significantly reduce the number of cells dislodged from printed grafts when compared to our previous approaches utilizing hyaluronic acid to facilitate cell attachment. The thrombin bath also maintains graft hydration and is warmed to 37° C in efforts to limit cell stress during printing. When printing is complete, the bath is lowered to allow access to the temporary frame for transfer to a culture plate.

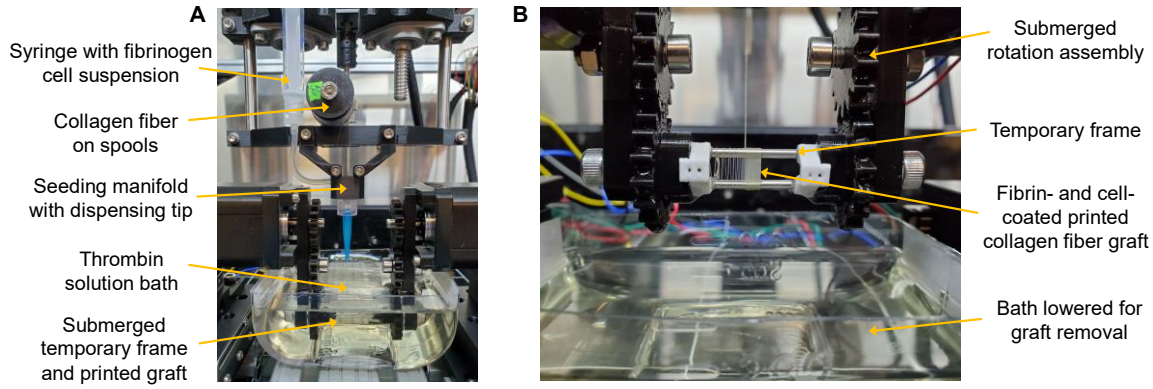

Figure 12. Submerged fibrin-based bioprinting approach. (A) Photo of the custom printhead and collection assembly where collagen fiber is coated with a fibrinogen cell suspension and crosslinked in a thrombin bath to form 3D grafts. (B) Close-up of the submerged rotation assembly and printed graft on a temporary frame, after lowering the thrombin bath.

We assessed the attachment and growth of hMSCs in fibrin grafts over 7 days to confirm the feasibility of the printing approach. Fluorescence imaging with DiD (green) and fiber autofluorescence (blue) shows grafts with hMSCs distributed throughout after 7 days in culture (**Figure 13**). Cells elongated parallel to the fiber direction, maintained high viability, and underwent rapid proliferation, indicating that the submerged fibrin-based printing process is feasible and offers significant advantages over previous approaches. The printing process and design were finalized and will be used to complete the remaining grant studies.

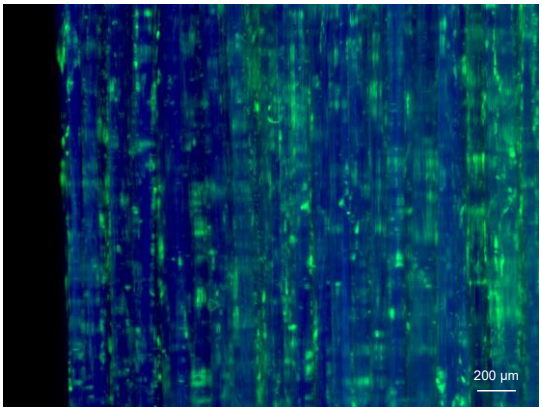

Figure 13. Microscopic fluorescence image of a graft printed using the submerged fibrin-based approach after 7 days in culture. Cells (hMSCs) are shown with the cytoplasmic label DiD (green) and collagen fiber with autofluorescence at 405 nm (blue). The graft edge can be seen at the far left of the image, with black background.

7. Assessment of tissue development during bioreactor culture

With the printing process finalized, we completed a 14-day study to assess synthetic tissue development of cellularized grafts undergoing cyclic strain in bioreactor culture for comparison with unconstrained culture in well plates. Grafts were printed with hMSCs using the process and conditions described above and secured into bundles using 6-0 Prolene suture.

For culture under cyclic strain, grafts (n=6) were loaded into our bioreactor with custom mounting fixtures (**Figure 7**). Using optimized conditions, grafts were subject to 2.5% strain (0.175 mm travel) at a grip travel rate of 0.1 mm/s in a triangle wave pattern. Cycling alternated continuously with a pattern of 3 hours on and 3 hours off. For unconstrained culture, identical grafts (n=6) were kept free-floating in low cell binding sterile well plates. Media was exchanged from both groups every 3-4 days.

Cell metabolic activity was assessed periodically for bioreactor grafts and unconstrained grafts. The alamarBlue assay is a means to quantify the metabolic activity of cells and is nondestructive, such that a group of printed grafts can be tested at multiple timepoints and returned to culture for later assessment. This ability is critical for complex, costly, and time-consuming bioreactor studies, as running destructive tests which do not allow for continuation to further timepoints would not be feasible.

While cell metabolic activity is not directly indicative of cell number due to the possibility of varying cell states, alamarBlue has been used to estimate the total number of cells in a graft by generating a standard curve. Known numbers of cells were plated in a well plate using serial dilution, allowed 3 hours for attachment, and assessed using standard alamarBlue protocols. The generated curve (**Figure 14A**) shows the second order relationship between cell number and measured fluorescence intensity, fit with an R^2 value of 0.9937. From the generated equation, we can estimate the number of cells within grafts based on the measured fluorescence intensity.

Cell metabolic activity for both bioreactor grafts and unconstrained grafts was assessed at day 0 (immediately before beginning cyclic strain or unconstrained culture) and after 3, 7, and 14 days of culture (**Figure 14B**). Using standard curves, the total number of cells per graft over time can be estimated (**Figure 14C**).

Notably, unconstrained grafts showed a significantly larger increase in metabolic activity and number of cells per graft over 14 days of culture when compared to grafts cultured under cyclic strain in the bioreactor. Both bioreactor and unconstrained grafts began with a nearly identical average number of cells at ~1700 cells/graft each. After 14 days of culture, unconstrained grafts averaged 106,292 cells/graft while bioreactor grafts averaged 45,745 cells/graft. Interestingly, bioreactor grafts experienced a very gradual increase in cell number over the first 7 days followed by rapid proliferation from day 7 to 14.

From this we theorize that the cyclic strain protocol could be somewhat damaging to initial cell viability or is impacting cell behavior in a way which delays or reduces proliferation. Based on our bioreactor optimization and published literature, we do not expect the strain protocol to significantly reduce cell viability. Thus, bioreactor culture may be promoting strain-induced changes in hMSC phenotype, such as inducing tenogenic differentiation and a delayed or reduced rate of proliferation. Upcoming studies assessing the effects of cyclic strain on gene expression and cell morphology will offer valuable insight into this. These assessments will be conducted on bioreactor and unconstrained grafts from this study which were snap frozen at the conclusion of the 14-day culture period, as well as grafts from additional upcoming bioreactor runs.

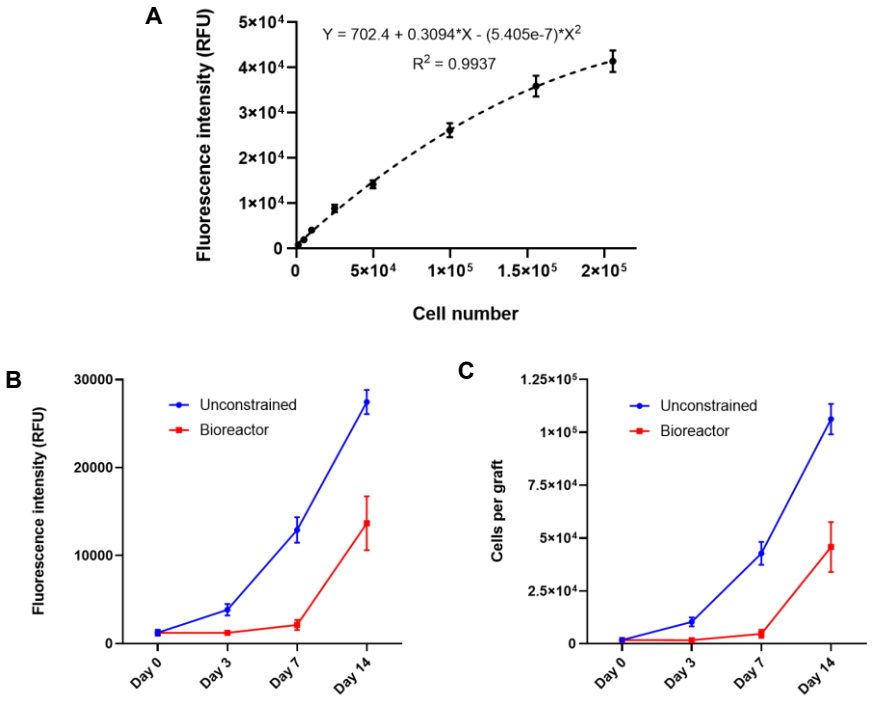

Figure 14. Metabolic activity and cell number of bioprinted grafts undergoing cyclic strain bioreactor culture and unconstrained static culture. (A) Standard curve showing the relationship between cell number and fluorescence intensity measured using the alamarBlue assay. (B) Fluorescence intensity of unconstrained and bioreactor culture groups over a 14-day culture period. (C) Estimated number of metabolically active cells per graft of unconstrained and bioreactor culture groups over a 14-day culture periods.

8. Assessment of tissue regeneration in MTJ defect model

Planned collaborative work with Old Dominion University (ODU) including manufacture and implantation of bioprinted grafts in the rodent model was significantly delayed by mandatory university shutdowns spanning more than 9 months in response to COVID-19. Specifically, required lab space and animal facilities were inaccessible and animal research protocols required resubmission and reapproval as policies changed throughout the year. In light of these delays, a no-cost extension was requested and granted for completion of all initially proposed work within an extension period of 12 months.

As facility availability returned to normal mid-2021, we began a small pilot study using subcutaneous implants to finalize AC-DC graft composition for the MTJ defect model. Three experimental groups were produced: Grafts of only collagen fiber, grafts of collagen fiber with HA as a matrix, and grafts of collagen fiber with fibrin as a matrix (n=8 each) (**Figure 15**). After printing, grafts were secured at each end with 6-0 Prolene suture with needles retained to facilitate surgical attachment. Grafts were implanted subcutaneously and harvested after 21 days in life along with rodent hind limbs. Hind limbs will be used to develop appropriate mounting fixtures to facilitate uniaxial tensile testing of the Achilles-MTJ region for upcoming studies as well as generate baseline unoperated control data. Histological assessment and scoring are underway and will allow us to move forward with an optimal graft composition.

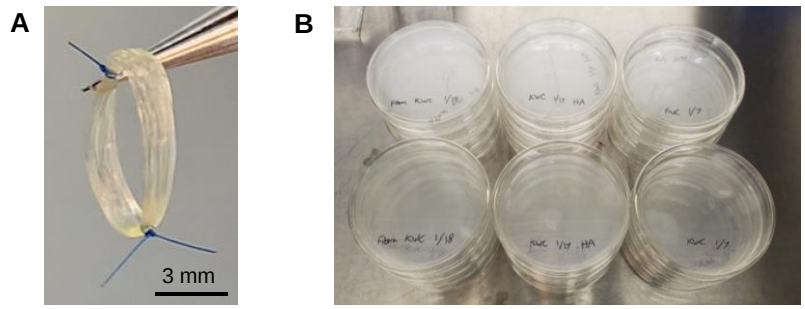

Figure 15. Bioprinted grafts prepared for implantation in rodents. (A) A standard graft to be used in our studies illustrating graft dimensions and the location of attachments with suture. (B) Grafts stored in sterile 90 mm dishes for transportation to animal facilities.

What opportunities for training and professional development has the project provided?

The project provided several opportunities for training and professional development for primary contributors to the project as well as interns. Researchers gained greater proficiency from interdisciplinary technical training by colleagues from varying backgrounds spanning chemistry, biology, and mechanical/biomedical engineering. Further knowledge and skills were developed by attending conferences and symposiums, both in person (4th Annual Mid-Atlantic Advanced Biomanufacturing Symposium, University of Virginia, VA) and online (AM Medical Virtual Summit, 3DHEALS2020 Virtual Webinar, and ORS 2021) due to COVID-19.

How were the results disseminated to communities of interest?

Results achieved from this project were disseminated to the biofabrication community as well as the general public at the 4th Annual Mid-Atlantic Advanced Biomanufacturing Symposium at the University of Virginia, with our poster winning first place in the associated competition. Our work was also submitted and accepted for poster presentation at the 2020 Military Health System Research Symposium (MHSRS) and resubmitted and accepted for podium presentation at the 2021 MHSRS, but both conferences were later canceled due to COVID-19. Our work developing biomanufactured cell-decorated collagen fiber grafts was also accepted for both podium and poster presentations at the Orthopaedic Research Society 2021 Annual Meeting, and selected as a finalist for the New Investigator Recognition Award. A manuscript titled “Assembled Cell-Decorated Collagen (AC-DC) bioprinted implants mimic musculoskeletal tissue properties and promote functional recovery” which details much of our progress and results is currently under review at Advanced Healthcare Materials as of August 11th, 2021. This manuscript has been made available pre-print via bioRxiv at: https://doi.org/10.1101/2021.06.22.449431.

What do you plan to do during the next reporting period to accomplish the goals?

1. Validate protocols for assessment of gene expression and complete additional culture periods using the cyclic strain bioreactor to assess synthetic tissue development.

2. Complete histological analysis of pilot study implants to finalize graft characteristics and develop a mechanical testing setup/protocols for determining Achilles-MTJ tissue properties.

3. Produce grafts and begin implantation for the MTJ defect model to study graft performance and tissue regeneration *in vivo*.

4. IMPACT:

What was the impact on the development of the principal discipline(s) of the project?

A novel biomanufacturing, or three-dimensional (3D) bioprinting, approach was developed which offers a significant contribution to the state of the art in tissue engineering technology. This process is capable of producing living tissue-like grafts from strong clinical-grade collagen fibers and human cells. These grafts are made with customized geometries and mimic key biological, material, and functional properties of native musculoskeletal tissue with significant advantages over past tissue engineering approaches. It's envisioned that this platform technology can produce cellularized grafts on-demand which promote and accelerate regeneration and functional recovery in debilitating musculoskeletal tissue injuries. Additionally, methods to characterize and quantify the properties of bioprinted grafts *in vitro* were developed. These approaches may aid in standardizing the assessment of properties across the tissue engineering field, which has traditionally often relied of qualitative or subjective methods.

What was the impact on other disciplines?

While still in development, the biomanufacturing technology platform and resulting biomimetic grafts prospectively offer the potential to drastically improve the treatment paradigm for musculoskeletal tissue injuries. Foreseeably, the adoption of functional bioprinted grafts by surgeons and care providers eliminates challenges associated with current treatment options and may lead to significantly improved patient outcomes for Warfighters and civilians alike.

What was the impact on technology transfer?

As a biotechnology start-up company, we are currently developing the technology and working toward commercialization. With further development, the technology could foreseeably be adopted by various government or industry biomanufacturing research, development, and manufacturing operations.

What was the impact on society beyond science and technology?

While still requiring significant development and commercialization, biomanufactured grafts prospectively offer next-generation treatments for the millions of Americans suffering from musculoskeletal tissue injuries each year. This can translate to significantly improved patient outcomes by accelerating or facilitating the return to activity, as well as possible improved efficacy, logistics, and economic benefits to the healthcare system as a whole. AC-DC implants may potentially accelerate and facilitate functional tissue regeneration in injured Warfighters with debilitating injuries, which could otherwise significantly delay or entirely prevent return to duty or even daily life.

5. CHANGES/PROBLEMS:

Changes in approach and reasons for change

Nothing to report.

Actual or anticipated problems or delays and actions or plans to resolve them

All animal-related work was delayed due to the COVID-19 global pandemic. Specifically, collaborating university laboratories and animal facilities were inaccessible for several months. In light of this, we requested and were granted a 12-month no cost extension during which we will complete all originally proposed work. We resumed animal work as the required facilities became available and operating normally recently, and expect to maintain access to these facilities for the remainder of the project.

Changes that had a significant impact on expenditures

In line with delayed animal-related work due to mandatory COVID-19 shutdowns, related expenditures have also been delayed. This has led to significantly reduced expenditure from what was projected. While substantial progress was still made regarding technology development, expenditures allocated specifically to the animal study have been delayed. We have recently resumed animal-related work and expect to remain on track with initial budget estimates as we complete the originally proposed work.

Significant changes in use or care of human subjects, vertebrate animals, biohazards, and/or select agents

Significant changes in use or care of human subjects

Nothing to report.

Significant changes in use or care of vertebrate animals

Nothing to report.

Significant changes in use of biohazards and/or select agents

Nothing to report.

6. PRODUCTS:

- **Publications, conference papers, and presentations**

Journal publications.

Nothing to report.

Books or other non-periodical, one-time publications.

Nothing to report.

Other publications, conference papers and presentations.

Poster presentation at the 4th Annual Mid-Atlantic Advanced Biomanufacturing Symposium at the University of Virginia, VA.

Abstract accepted for poster presentation at the 2020 Military Health System Research Symposium (later canceled due to COVID-19).

Poster and podium presentation at 2021 Orthopaedic Research Society Annual Meeting (virtual) with recognition as a New Investigator Recognition Award finalist.

Abstract accepted for podium presentation at the 2021 Military Health System Research Symposium (later canceled due to COVID-19).

- **Website(s) or other Internet site(s)**

Nothing to report.

- **Technologies or techniques**

A novel biomanufacturing, or three-dimensional (3D) bioprinting, platform technology and related techniques were developed. Currently, the technology and process remain in-house only.

- **Inventions, patent applications, and/or licenses**

Submission of two PCT patent applications describing inventions developed from our research:

1. A 3D bioprinting process utilizing a rotating frame to form cellularized composite collagen fiber-based grafts. “Francis M, Christensen K. 2020. Rotating frame apparatus and composite biological scaffold. U.S. Provisional Patent Application Serial No.: 63/119,628.”

2. A 3D bioprinting process utilizing a micropost array to form cellularized composite collagen fiber-based grafts. “Micropost array apparatus and composite biological scaffold. U.S. Provisional Patent Application Serial No.: 63/119,618.”

- **Other Products**

A novel biomanufacturing, or three-dimensional (3D) bioprinting, platform technology and related techniques were developed. It’s envisioned that this technology can produce cellularized grafts on-demand which promote regeneration and functional recovery in musculoskeletal tissue injuries.

7. PARTICIPANTS & OTHER COLLABORATING ORGANIZATIONS

What individuals have worked on the project?

Name:	Dr. Kyle Christensen
Project Role:	Principal investigator
Researcher Identifier (ORCID ID):	0000-0001-6981-4676
Nearest person month worked:	24
Contribution to project:	Project lead with emphasis and expertise on process design, engineering, and experimental validation.
Name:	Dr. Michael Francis
Project Role:	(Previous Principal Investigator)
Researcher Identifier:	991506
Nearest person month worked:	6
Contribution to project:	Project guidance with expertise and emphasis on biological characterization and clinical relevance
Name:	Dr. Anna Bulysheva
Project Role:	Collaborating Professor
Researcher Identifier:	NA
Nearest person month worked:	6
Contribution to project:	Conduct animal work at Old Dominion University including study development, surgeries, and analysis.

Has there been a change in the active other support of the PD/PI(s) or senior/key personnel since the last reporting period?

The previous PI (Dr. Michael Francis) will no longer have involvement with the project and Dr. Kyle Christensen will step in as the new PI. As the primary contributor to this work, Dr. Christensen is excellently positioned to ensure the completion of all originally proposed goals of this project. Accordingly, updated documentation including Current and Pending Support, Statement of Work, and Biosketch have been submitted to the Grants Administrator to facilitate processing this change in PI.

What other organizations were involved as partners?

Organization Name: Old Dominion University (ODU)
Location of Organization: Norfolk, VA
Partner's contribution to project: ODU animal facilities will be used for all animal work and related analysis will be completed in the ODU laboratory of Dr. Anna Bulysheva.

8. SPECIAL REPORTING REQUIREMENTS

Quad Chart is attached with the submission.

9. APPENDICES:

Three journal articles are attached with the submission as Appendices A, B, and C, and referenced in the text.